The Stability and Passivity of MOSFET Device Models That Use Nonreciprocal Capacitive Elements

LANCE A. GLASSER

Abstract—**We examine the activity and stability of circuits built from device models formed by a linear active or passive multiport resistor in parallel with a positive definite, but nonreciprocal, multiport capacitor. Numerical range methods are used to determine the maximum frequency of oscillation and maximum exponential growth rate of the solutions for both conservation of real power and conservation of complex power. We also examine the stability and activity of these devices when a positive-definite multiport resistor is added in series. It is shown that with the inclusion of the resistor, the circuit becomes passive at high frequencies even if the capacitor is nonreciprocal. The implications of these results for MOSFET device modeling are discussed.**

I. Introduction

IN THIS PAPER, we will investigate linear models for active multiport circuit elements in light of recent modeling trends, which include the use of nonreciprocal reactances in device models. Several trends in device models for circuit simulation are evident. The first point is that for applications such as VLSI the dynamics of the intrinsic device tend to be dominated by extrinsic circuit parasitics. For instance, although there has been a continuing effort to develop accurate MOSFET capacitance models, especially for analog circuit design, it can be argued that, in most applications, it is much more important to model accurately such extrinsic elements as the resistance of lightly doped drains, overlap capacitances, and interconnect capacitors and resistors. Second, there is a high premium on developing a model that is easily applicable to large-signal analysis. Thus, although many sophisticated linear *RC* transmission line models were developed for MOSFET's in the 1960's [1]–[5], the most widely used MOSFET models today consist of a nonlinear multiport resistor in parallel with a nonlinear multiport capacitor. These models are particularly well suited for incorporation into large-signal circuit simulators. The Meyer model [6] is an example of such a simulation-oriented model and, even in this simple case, there have been problems stemming from the nonlinearity of the reactance. Third, we have seen the emergence of a new type of model, a model with asymmetric linear reactances. Such models are widely used for MOSFET's [7] and are also important in superconducting field-effect transistors [8]. The issue of nonreciprocal linear reactances is the focus of this paper.

We return to linear circuit theory to examine the general small-signal behavior of some large-signal intrinsic device models now in use. The viewpoint taken herein is that when pushed to their fundamental limits, the behavior of device models is important because circuit designers often use device models to explore the potential of unusual circuit configurations. It can be very misleading to have an intrinsic device model that shows anomalously fantastic behavior in an unconventional configuration. True, this anomalous behavior may mostly disappear when a ponderous network of extrinsic parasitics is added to the device, but circuit intuition, and perhaps accuracy, suffers. Of course, there are many criteria for comparing the merits of competing models. For instance, MOSFET capacitance models typically are judged with respect to charge conservation, the accuracy of the reactance compared with more distributed models, and the accuracy compared with manufactured devices. These important issues are largely beyond the scope of this paper, which primarily considers the importance of nonreciprocal reactive elements in MOSFET device models.

II. Theoretical Approach

The theoretical approach is based on numerical range concepts. Numerical range methods recently have been used to determine tight bounds on the natural frequencies of sets of linear networks [9]. In this paper, we use numerical range concepts to examine the resistive embedding of nonreciprocal reactive multiports with respect to activity and stability. The technique is very general, applying, for instance, to an active nonreciprocal capacitor embedded in an active nonreciprocal multiport resistor. The approach has a geometric flavor.

Following our previous work, we apply the law of conservation of complex power in the Laplace transform domain, where $s = \sigma + j\omega$ is the complex frequency variable. The devices under consideration are linear time-invariant n-ports described by means of their admittance

Manuscript received December 8, 1988; revised August 21, 1989. This paper was recommended by Associate Editor C. A T. Salama.

The author was with the Central Research Laboratory, Hitachi, Ltd., Kokubunji, Tokyo, Japan. He is now with the Defense Advanced Research Projects Agency, Arlington, VA 22209.

IEEE Log Number 9034904.

matrices in accordance with

$$i(s) = Y(s)v(s) \tag{1}$$

where $Y(s) \in C^{n\times n}$ is the port admittance matrix, and $v(s) \in C^n$ and $i(s) \in C^n$ are the vectors of port voltages and currents, respectively. The complex power $p(s)$ entering the n-port is given by the quadratic form

$$p(s) = v^{H}(s)i(s) = v^{H}(s)Y(s)v(s) \tag{2}$$

where $v^{H}(s)$ denotes the complex conjugate transpose of $v(s)$.

In this paper, we look at two general properties of networks that can be built out of the preceding devices—the stability, characterized by the location of the natural frequencies, and passivity of the final circuit. These properties are related but not identical. A circuit can be active (not passive) but contain no right-half-plane natural frequencies. The difference comes about because passivity addresses the question of whether unbounded power can be extracted with the correct excitation, whereas stability addresses the question as to whether the allowable modes can grow. The stability case is more restrictive, since there are no sources to help match boundary conditions. To examine activity, we invoke conservation of real power; to examine stability, we invoke the more restrictive concept of conservation of complex power.

We express our results in terms of the numerical range of $Y(s)$. Facts about the numerical range of matrices are given in the Appendix of [9].

Definition 1: Let S_C be the unit sphere in C^n defined by $S_C \triangleq \{x \in C^n | x^H x = 1\}$. For any square matrix $A \in C^{n\times n}$, the numerical range of A, $W(A)$, is defined by $W(A) \triangleq \{x^H A x | x \in S_C\}$.

Combining theorems 1 and 4 of [9], we have the following theorem.

Theorem 1: Let $\mathscr{N} \triangleq \{\mathscr{N}_1, \cdots, \mathscr{N}_M\}$ be any set of linear time-invariant multiports, not necessarily all of the same size, characterized by an associated set of admittance matrices $\mathscr{Y} \triangleq \{Y_1(s), \cdots, Y_M(s)\}$. Let $\{\mathscr{L}_1, \cdots, \mathscr{L}_N\}$ be any set of linear time-invariant multiports characterized by admittance matrices that are positive scalar multiples of matrices from the set $\mathscr{Y}$; i.e., for each $i \in \{1, \cdots, N\}$, the admittance matrix $\mathscr{L}_i$ is of the form $a_i Y_{K(i)}(s)$, where $a_i \in R$ is positive and $K(\cdot)$: $\{1, \cdots, N\} \to \{1, \cdots, M\}$. Define

$$Y(s) \triangleq \operatorname{diag}\{Y_1(s), \cdots, Y_M(s)\}. \tag{3}$$

For $s_0 \in C$, a complex frequency not a pole of $Y(s)$, a circuit that has s_0 as a natural frequency and is formed by interconnecting $\mathscr{L}_1, \cdots, \mathscr{L}_N$ using only ideal (multiwinding) transformers and ideal connecting wire exists iff $0 \in W(Y(s_0))$.

Theorem 1 motivates the following classifications of sets of linear devices.

Definition 2: We say a set of uniquely solvable linear time-invariant devices $\mathscr{S}$, as defined in Theorem 1, is *stable* if for every complex frequency s_0 in the open right-half s plane, $0 \notin W(Y(s_0))$. We abbreviate this by saying that $Y(s)$ is stable. It will sometimes be convenient to talk about a frequency interval over which $Y(s)$ is stable. That is, we say that $\mathscr{S}$ is stable over the frequency interval Ω if for every $\omega_0 \in \Omega$ and $\sigma_0 > 0$, $0 \notin W(Y(\sigma_0 + j\omega_0))$. If $Y(s)$ is not stable, it is *unstable*.

In other words, all networks composed of ideal wire, ideal transformers, and the elements of $\mathscr{S}$, taken in any multiplicity and impedance scaled by any positive real number, have voltage and current solutions that either decay exponentially to zero, are sinusoidal, or are constant, if there are no possible natural frequencies of any of these networks that have exponentially growing modes ($\sigma_0 > 0$). Note that we are looking at the stability of not just one network, but a whole class of networks.

Definition 3: We say a set of uniquely solvable linear time-invariant devices $\mathscr{S}$, as defined in Theorem 1, is passive if for every complex frequency s_0 in the open right-half s plane, $Y_H(s_0)$ is positive definite, where $Y_H(s_0)$ is the Hermitian part of $Y(s_0)$. We abbreviate this by saying that $Y(s)$ is passive. If $Y(s)$ is not passive, it is *active*.

In other words, all networks composed of ideal wire, ideal transformers, and the elements of $\mathscr{S}$, taken in any multiplicity and impedance scaled by any positive real number, are passive if for all $\sigma_0 > 0$, $Y(\sigma_0 + j\omega)$ is positive definite or, equivalently, if $W(Y(\sigma_0 + j\omega))$ lies entirely in the open right half-plane. (When we say that a non-Hermitian matrix A is "positive definite," we mean that its Hermitian part $A_H = (A + A^H)/2$ is positive definite.)

Our definitions of stability and passivity are typical of those used to describe linear networks, with the important exception that Definitions 2 and 3 apply to classes of networks rather than to specific networks.

Theorem 2: If a set of linear time-invariant devices $\mathscr{S}$, as defined in Theorem 1, is passive, then it is *stable*. If it is *unstable*, then it is *active*.

Generally speaking, activity is examined by looking at the Hermitian part of $Y(s)$ and instability by looking at both the Hermitian and anti-Hermitian parts of $Y(s)$. It is useful to parameterize the real and imaginary frequencies for which $0 \in W(Y(s))$ (the condition for instability) and $0 \in W(Y_H(s))$ (the condition for activity) by four physically meaningful numbers. We have

$$\sigma_{\max\text{-unstable}}(\omega) \triangleq \max_{\sigma}\{\sigma \in R | 0 \in W(Y(\sigma + j\omega))\} \tag{4}$$

$$\sigma_{\max\text{-active}}(\omega) \triangleq \max_{\sigma}\{\sigma \in R | 0 \in W(Y_H(\sigma + j\omega))\} \tag{5}$$

$$\omega_{\max\text{-unstable}} \triangleq \max_{\omega}\{\omega \in R | 0 \in W(Y(0 + j\omega))\} \tag{6}$$

$$\omega_{\max\text{-active}} \triangleq \max_{\omega}\{\omega \in R | 0 \in W(Y_H(0 + j\omega))\}. \tag{7}$$

The parameter $\sigma_{\max}$ describes the maximum exponential growth rate of the envelope of the circuit modes, and

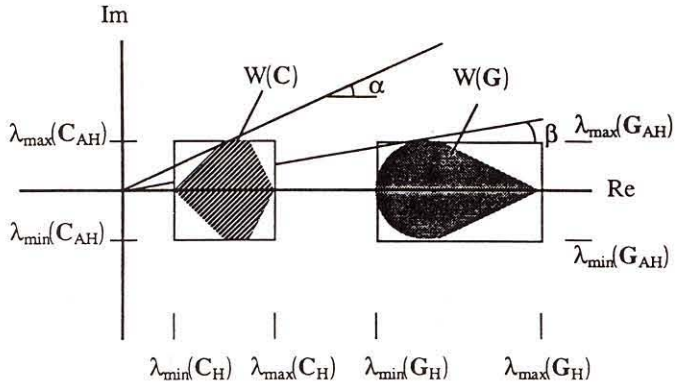

Fig. 1. Numerical range of two positive-definite nonsymmetric real matrices G and C. The maximum and minimum eigenvalues, λ_{min} and λ_{max}, of these two matrices are also shown. The rectangles in the figure are bounds on $W(G)$ and $W(C)$. They are used in Section V.

ω_{max} characterizes the maximum sinusoidal frequency of oscillation [10]. In a circuit context, σ_{max} might be used to characterize the speed at which voltages in a bistable latch or comparator leave the region of the metastable point. There are two varieties of each parameter, depending on whether we require conservation of complex power (leading to $\sigma_{max-unstable}$ and $\omega_{max-unstable}$) or just conservation of real power (leading to $\sigma_{max-active}$ and $\omega_{max-active}$).

III. Devices with a Positive Definite Conductance Matrix

In this and the next section, we examine devices consisting of a multiport resistor in parallel with a multiport capacitor. This device is a generalization of the transistor model considered by Thornton [11]. This device can be described by an admittance matrix of the form

$$Y(s) = sC + G \tag{8}$$

where $C, G \in R^{n\times n}$, and C is the capacitance matrix and G the conductance matrix. In this section, both G and the capacitance C are positive definite. Because C and G are real, their numerical ranges $W(C)$ and $W(G)$ are symmetric about the real axis, as shown in Fig. 1. The maximum and minimum eigenvalues λ of the Hermitian and anti-Hermitian parts of G and C are also shown. (The anti-Hermitian part of G is $G_{AH} = (G - G^H)/2$.)

The behavior of $W(Y(s))$ determines the stability and activity of the set of n-ports. For $s = \sigma \geq 0$, $W(sC)$ forms a cone in the closed right half-plane, directed to the right, as shown in Fig. 2. The cone is given by $W_1 \triangleq \{\sigma z | \sigma \geq 0$ and $z \in W(C)\}$. By a simple inequality [12],

$$W(\sigma C + G) \subseteq W_2 \triangleq W_1 + W(G). \tag{9}$$

Fig. 3 illustrates W_2. Clearly, $\sigma C + G$ is positive definite for all $s = \sigma \geq 0$.

For $s = j\omega$ with $\omega \geq 0$, $W(sC)$ forms a cone in the nonnegative imaginary half-plane, directed up, as shown in Fig. 4. The cone is defined by $W_3 \triangleq \{j\omega z | \omega \geq 0$ and $z \in W(C)\}$. When C is symmetric, $C_{AH} = 0$ and W_3 is a ray consisting of the nonnegative imaginary axis. For $C_{AH} \neq 0$, $W(Y(j\omega)) \subseteq W_3 + W(G)$; $Y(s)$ is positive definite when σ

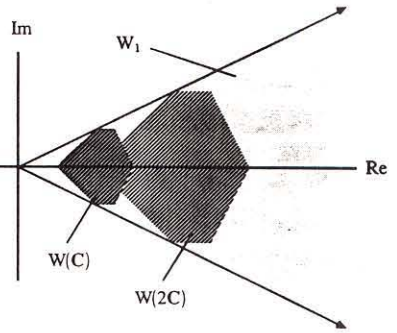

Fig. 2. Set $W_1 = \{\sigma z | z \in W(C)$ and $0 \leq \sigma \in R\}$.

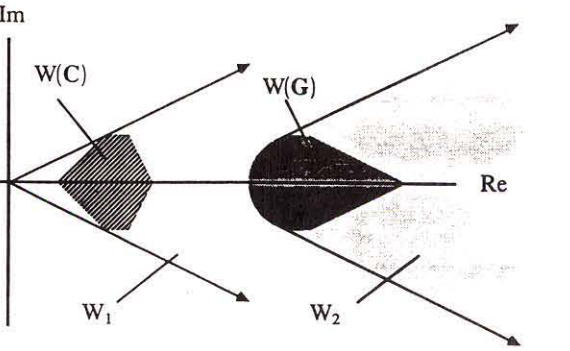

Fig. 3. Set $W_2 = \{x + \sigma z | z \in W(C)$, $x \in W(G)$, and $0 \leq \sigma \in R\}$. W_2 is a bound on $W(G + \sigma C)$ for $\sigma \geq 0$.

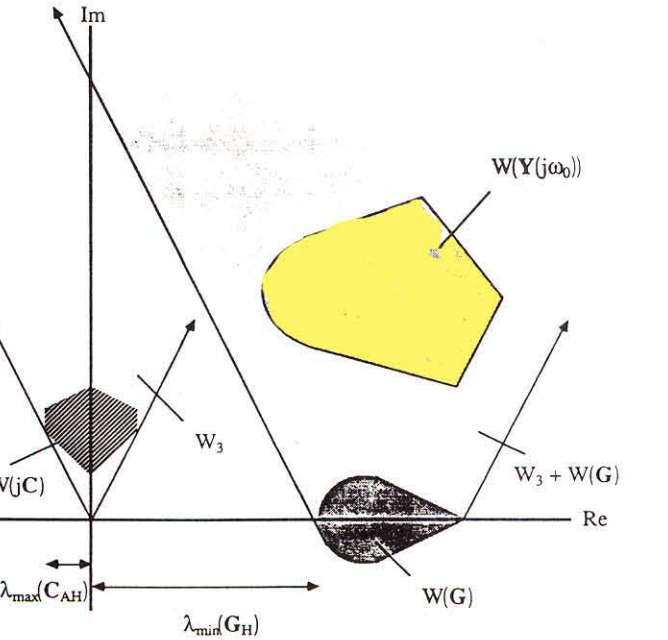

Fig. 4. Set $W_3 = \{j\omega z | z \in W(C)$ and $0 \leq \omega \in R\}$. W_3 is a bound on $W(j\omega C)$ for $\omega \geq 0$. Set $W(G + j\omega C) \subseteq \{x + j\omega z | z \in W(C)$, $x \in W(G)$, and $0 \leq \omega \in R\}$. $W_3 + W(G)$ is a bound on $W(G + j\omega C)$ for $\omega \geq 0$. A possible set $W(G + j\omega C)$ is shown.

≥ 0 and $|\omega| \leq \omega' = \lambda_{min}(G_H)/\lambda_{max}(jC_{AH})$. Note that for a matrix A, $W(A_H) = [\lambda_{min}(A_H), \lambda_{max}(A_H)]$ and $jW(A_{AH}) = [\lambda_{min}(jA_{AH}), \lambda_{max}(jA_{AH})]$. If C is not symmetric, it is possible for $Y(s)$ to be unstable at frequencies above ω'. Even when $Y(s)$ is stable, it is possible for the Hermitian part of $Y(s)$ to become indefinite. For questions of activity, we need look only at the Hermitian part of (8),

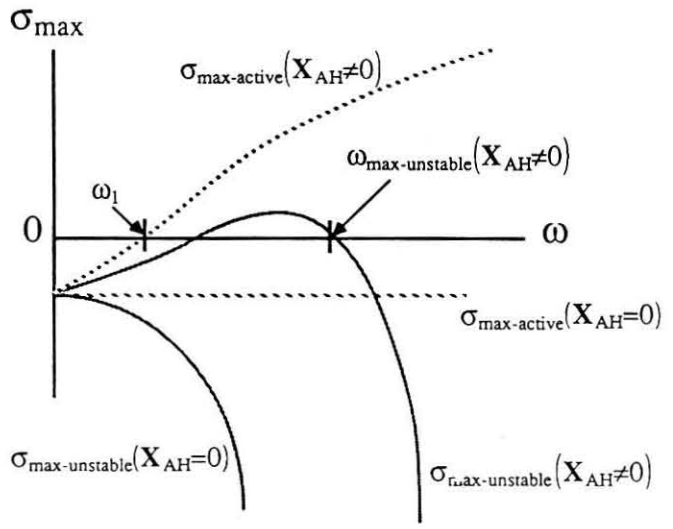

Fig. 5. General behavior of the exponential constants $\sigma_{\max\text{-active}}$ and $\sigma_{\max\text{-unstable}}$ versus frequency ω for a parallel connection of positive definite capacitance C with a positive definite conductance G. Note that both $\sigma_{\max\text{-active}}$ and $\sigma_{\max\text{-unstable}}$ can be positive when C is nonreciprocal.

$$Y(\sigma + j\omega) = G_{\mathrm{H}} + \sigma C_{\mathrm{H}} + j\omega C_{\mathrm{AH}}. \tag{10}$$

The general frequency behavior of the model in (8) can be easily derived from the properties of the numerical range. The form of the results is shown in Fig. 5. We will not go through the details, but the general form of the behavior can be found with the help of the following observations:

$$\begin{aligned} 0 \in W(Y(s)) &\Rightarrow 0 \in W(G) + sW(C) \\ &\Rightarrow W(-G) \cap sW(C) \neq \varnothing \end{aligned} \tag{11}$$

where we note that $W(-G) = -W(G)$. We also observe that

$$\begin{aligned} &\lambda_{\min}(G_{\mathrm{H}}) + \lambda_{\min}(\sigma C_{\mathrm{H}} + j\omega C_{\mathrm{AH}}) \\ &\leqslant \lambda_{\min}(Y_{\mathrm{H}}(s)) \leqslant \lambda_{\min}(G_{\mathrm{H}}) + \lambda_{\max}(\sigma C_{\mathrm{H}} + j\omega C_{\mathrm{AH}}) \end{aligned} \tag{12}$$

and

$$\begin{aligned} &\lambda_{\min}(G_{\mathrm{H}}) + \lambda_{\min}(\sigma C_{\mathrm{H}} + j\omega C_{\mathrm{AH}}) \\ &\leqslant \lambda_{\min}(Y_{\mathrm{H}}(s)) \leqslant \lambda_{\max}(G_{\mathrm{H}}) + \lambda_{\min}(\sigma C_{\mathrm{H}} + j\omega C_{\mathrm{AH}}) \end{aligned} \tag{13}$$

where we note that $W(A_{\mathrm{H}}) = \mathrm{Re}\{W(A)\} = [\lambda_{\min}(A_{\mathrm{H}}), \lambda_{\max}(A_{\mathrm{H}})]$. The matrix $Y(s)$ represents an active set of devices if $\lambda_{\min}(Y_{\mathrm{H}}(s_0)) < 0$ for $\mathrm{Re}\, s_0 > 0$.

With the help of (11) we can see that for $Y(s)$ to be unstable (i.e., $\omega_{\max\text{-unstable}}$ to exist in Fig. 5), we need $\alpha + \beta \geqslant \pi/2$, where α and β are the angles shown in Fig. 1. As another example, by setting $\sigma = 0$, (13) and $\lambda_{\min}(jC_{\mathrm{AH}}) = -\lambda_{\max}(jC_{\mathrm{AH}})$ (since $C \in R^{n\times n}$) lead to $\lambda_{\max}(G_{\mathrm{H}})/\lambda_{\max}(jC_{\mathrm{AH}}) \geqslant |\omega_1| \geqslant \lambda_{\min}(G_{\mathrm{H}})/\lambda_{\max}(jC_{\mathrm{AH}})$, where ω_1 is the frequency at which $Y(s)$ becomes active.

The graph in Fig. 5 expands on the well-known fact that nonreciprocal reactances are active. Take the specific example of a nonreciprocal capacitor. Taken by itself, this device is active at all frequencies. We see from Fig. 5 that if this capacitor is leaky (model the leakage by a parailel conductance), then the capacitor must be driven at high frequencies for the device to become active. Only if both the positive definite conductance and the positive definite capacitance are nonreciprocal can interconnections of these devices (see Theorem 1) be unstable.

It is worth emphasizing the difference between the preceeding theory, which, as it is a linear theory, addresses incremental properties, and the large-signal issues of passivity and stability. For instance, the Josephson junction, which has a current-flux relationship $i(t) = I_0 \sin K\phi(t)$, where I_0 and K are positive real constants and $v(t) = \dot{\phi}(t)$, is a lossless passive device in the sense of Wyatt *et al.* [13], [14]. At some operating points, however, it has a negative and reciprocal inductance. Hence, the Josephson junction is incrementally active at those operating points. In a large-signal sense, it absorbs power at some operating points and emits that power at other operating points—it all balances out.

IV. Devices with an Indefinite Conductance Matrix

For a MOSFET, G is active and so $Y(s)$ is unstable at $\omega = 0$. Because G is active, the important question is not whether or not modes can grow (they can), but rather how fast (i.e., $\exp(\sigma_{\max} t)$) and at what frequencies (i.e., below $\omega_{\max}$) they can grow. One suspects that for any good physical model, there should be a limit to the rate of growth of the circuit modes.

Fig. 6 illustrates the types of behavior one finds when G is active and C is positive definite. We see that for $C_{\mathrm{AH}} \neq 0$, $\sigma_{\max\text{-active}}$ increases with $|\omega|$, a quite nonphysical result. Note, however, that even when $C_{\mathrm{AH}} = \mathbf{0}$, $\sigma_{\max\text{-active}}$ does not decrease with frequency. This is not physical either, although less violently so. In both cases, $\omega_{\max\text{-unstable}}$ is finite as long as $0 \notin W(C)$.

We will now apply these results to MOSFET capacitance modeling. Because of its industrial importance, MOSFET capacitance modeling has been the subject of considerable research and the field is still active today [15]. Tsividis [16] presents an extensive bibliography. In this section, we generalize the thermodynamic arguments of Penfield [17] and compare the various models with respect to the reasonableness of the fundamental limits (e.g., $\sigma_{\max\text{-unstable}}$) that they predict. We also examine the accuracy of the lumped capacitance model with respect to multisection models.

For MOSFET models, G is the conductance matrix and C the capacitance matrix. Using the same notation as Paulos and Antoniadis [18], we have

$$\omega_0 = \mu(V_{GS} - V_T)/L^2 \tag{14}$$

and

$$\alpha = (V_{GD} - V_T)/(V_{GS} - V_T) \tag{15}$$

where ω_0 is the characteristic frequency of the device, μ the channel mobility, L the effective channel length, V_T the transistor threshold voltage, and $\alpha \in [0, 1]$ the saturation parameter. The linear region is defined by $\alpha \approx 1$, and

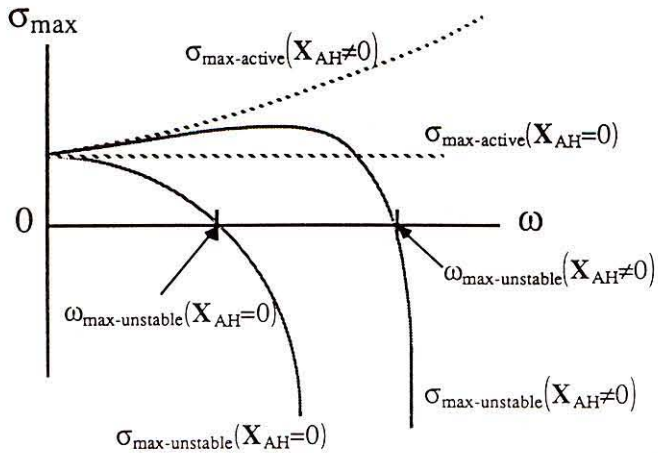

Fig. 6. General behavior of the exponential constants $\sigma_{max-active}$ and $\sigma_{max-unstable}$ versus frequency ω for a parallel connection of a positive definite capacitance C with an active conductance G. Note that even when C is reciprocal, $\omega_{max-active}$ is infinite.

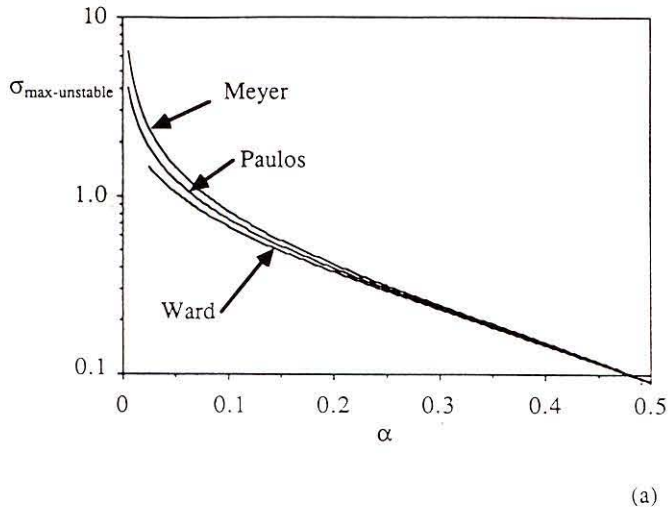

(a)

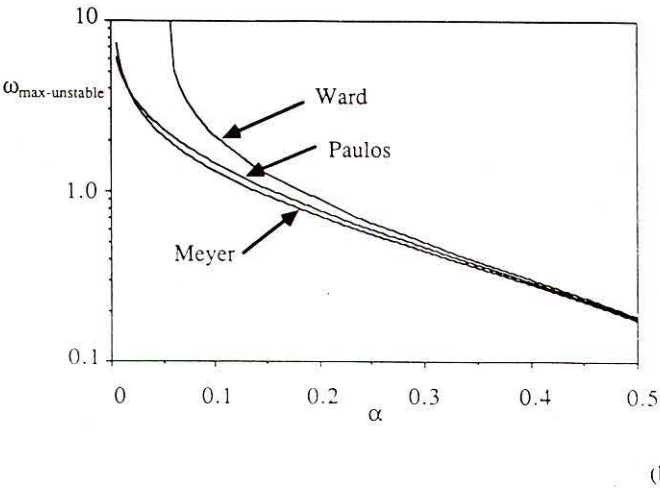

(b)

Fig. 7. Natural frequency limits (a) $\sigma_{max-unstable}$ and (b) $\omega_{max-unstable}$ versus the saturation parameter α. Both frequencies are normalized to ω_0 from (14).

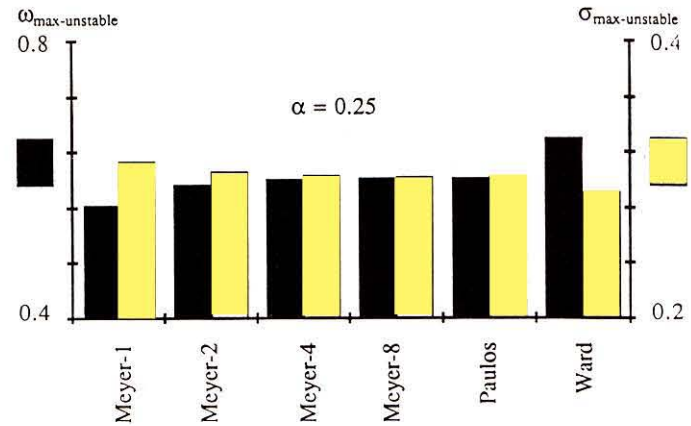

(a)

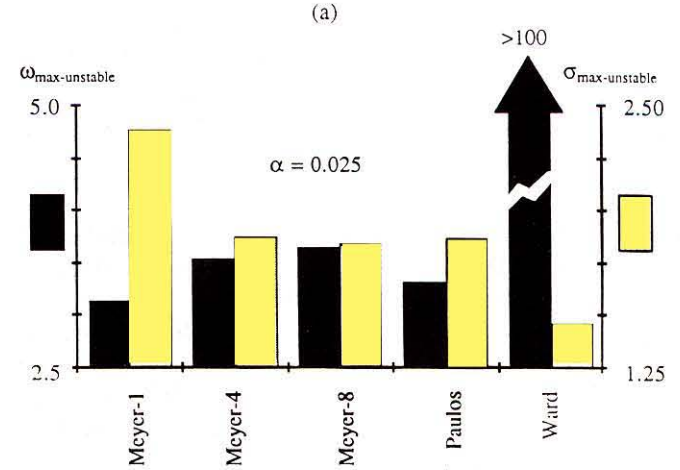

(b)

Fig. 8. Comparison of $\sigma_{max-unstable}$ and $\omega_{max-unstable}$ (normalized to ω_0) for the Paulos, Ward, and multisection Meyer models. (a) For the saturation parameter, $\alpha = 0.25$. (b) For the saturation parameter, $\alpha = 0.025$. The eight-section Meyer model, "Meyer-8," should be used as the standard against which the other models are compared.

saturation occurs as α approaches zero. In the remainder of the section, all real and imaginary frequencies are normalized to ω_0.

As α becomes large, the transistors become, qualitatively speaking, less active. Agreement among the values of σ_{max} and ω_{max} predicted by the Meyer [6], Ward [7], and Paulos [18] models becomes very close, as seen in Fig. 7. As α is decreased, differences emerge. Fig. 8(a) compares $\sigma_{max-unstable}$ and $\omega_{max-unstable}$ for six models at $\alpha = 0.25$. To provide a standard for comparison, one-, two-, four-, and eight-section Meyer models were used. In the multisection Meyer models, the transistor was partitioned into sections of equal voltage drop (the sections were shorter near the drain) and the Meyer model was applied to each section. Thus the eight-section Meyer model is a reasonable approximation of a distributed structure of the sort widely assumed to represent the true device. In the eight-section model, all device segments operate near the linear regime, where there is solid agreement on the

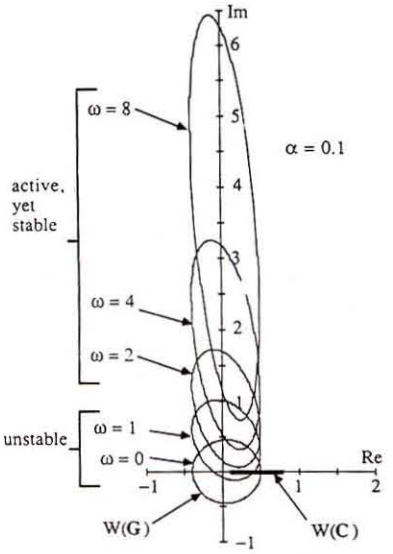

Fig. 9. Numerical range for the single-section Meyer model as a function of frequency at $\alpha = 0.1$. The numerical ranges of G and C are shown. Since C is symmetric and real, $W(C)$ is a line segment on the real axis. The normalized maximum frequency of oscillation is $\omega_{\max-\text{unstable}} = 1.31$.

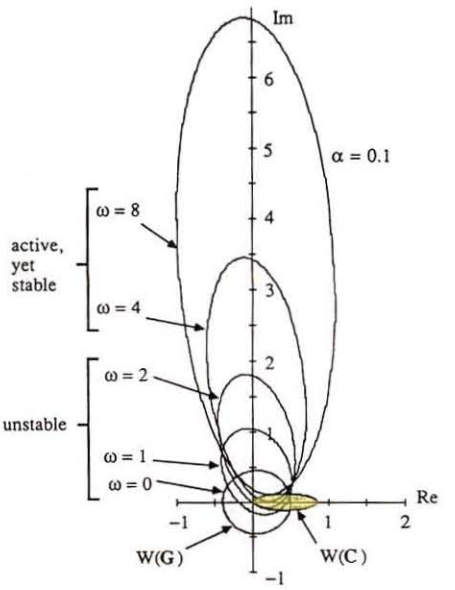

Fig. 10. Numerical range for the Ward model as a function of frequency at $\alpha = 0.1$. The numerical ranges of G and C are shown. Since C is real but not symmetric, $W(C)$ is an elliptical disk symmetric about the real axis. The normalized maximum frequency of oscillation is $\omega_{\max-\text{unstable}} = 2.094$.

device dynamics. This is why there is widespread confidence in the distributed model as a valid standard for comparison. As can be seen, the Paulos model is in excellent agreement with the multisection Meyer model at $\alpha = 0.25$. In Fig. 8(b), the models are evaluated very close to saturation, $\alpha = 0.025$. The Paulos model does fairly well, but the value of $\omega_{\max-\text{unstable}}$ predicted by the Ward model is optimistic by several orders of magnitude.

A qualitative appreciation for the behavior of the Meyer and Ward models can be obtained by examining the behavior of $W(Y(s))$. We will illustrate the numerical ranges of the Meyer, Ward, and Paulos models for $\alpha = 0.1$ and $\sigma = 0$. The (normalized) numerical values of $\omega_{\max-\text{unstable}}$ are 1.31, 2.09, and 1.46 for the Meyer, Ward, and Paulos models, respectively. Fig. 9 illustrates $W(Y(j\omega))$ for the Meyer model for ω (normalized to ω_0) from 0 to 8. Since C is reciprocal (symmetric), $\sigma_{\max-\text{1active}}(\omega)$ is constant at $\sigma_{\max-\text{active}}(0)$. As ω increases, the admittance becomes increasingly capacitive until, above $\omega_{\max-\text{unstable}}$, resonant circuits can no longer be built without inductors or equivalent devices. Conversely, $\omega_{\max-\text{active}}$ is infinite; the admittance always has a negative real part at $\sigma = 0$. Also shown in the figure is $W(G)$—an elliptical disk with foci at 0 and $g_D/(g_D + g_m)$—and $W(C)$—the real line segment [0.1, 0.8]. The plotted values of $W(Y(j\omega))$ lie within the bound $W(G) + j\omega W(C)$. (For the MOSFET, g_D is the output conductance and g_m the transconductance.) It can be shown, using the techniques illustrated in (11)–(13), that $\omega_{\max-\text{unstable}} \leq \lambda_{\max}(jG_{AH}/\lambda_{\min}(C_H)$. This bound is conservative by about a factor of three.

Fig. 10 illustrates the numerical range $W(Y(j\omega))$ for the Ward model. Note that $W(C)$ is no longer confined to the real axis because C is not symmetric. Therefore, $\sigma_{\max-\text{active}}$ increases with $|\omega|$, a quite nonphysical result. Note, however, that as long as C is positive definite, $\sigma_{\max-\text{unstable}}$ and $\omega_{\max-\text{unstable}}$ are both finite. For comparison, we show, in Fig. 11, $W(Y(j\omega))$ for the Paulos model, where the numerator and denominator of the elements of the admittance matrix are second order in s. For this reason, it is beyond the scope of the theory developed in this paper. Nevertheless, we see that $W(Y(j\omega))$ behaves in an intuitively pleasing manner at $\sigma = 0$, moving, as ω increases, from solutions that are unstable, to active, to $W(Y(j\omega))$ positive definite. Because we have not investigated $W(Y(s))$ at all $\sigma > 0$, we cannot yet say that the Paulos model does become stable at moderate frequencies and passive at high frequencies, as suggested by Fig. 11, but this would be an interesting point to prove eventually. It is certainly how one would like any reasonable

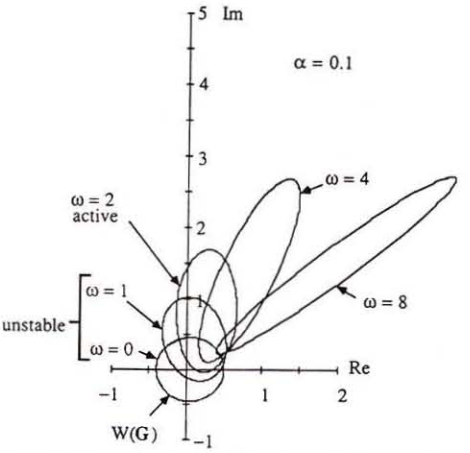

Fig. 11. Numerical range for the Paulos model as a function of frequency at $\alpha = 0.1$ and $\sigma = 0$. The normalized maximum frequency of oscillation is $\omega_{\max-\text{unstable}} = 1.46$. Note that the theory in this paper does not tell us about the stability and passivity of the Paulos model.

device model to behave.

V. Series/Parallel Embeddings of Stable Networks

In the previous section, we saw that, for instance, the parallel connection of an active n-port resistor and a reciprocal capacitor is active at all real frequencies ω. From the standpoint of predicting fundamental limits, these models are too simple. In this section, we look at series/parallel embeddings of the form

$$\boldsymbol{Z}(s) = \boldsymbol{K}^{-1}(s) + \boldsymbol{R} = (s\boldsymbol{C} + \boldsymbol{G})^{-1} + \boldsymbol{R} \tag{16}$$

where $\boldsymbol{C}$, $\boldsymbol{G}$, and $\boldsymbol{R} \in R^{n\times n}$. This model is sufficient to examine, for instance, the MOSFET of Section IV with series drain, gate, and source resistors. We will see that the high-frequency behavior of such models is much more reasonable.

The key issue is the effect of the inverse operation in (16) on the numerical range. Obviously, this numerical range can be computed for any given example, but what we want at this point is to discover its general behavior. To this end, we will look at bounds on $W((s\boldsymbol{C}+\boldsymbol{G})^{-1})$ given bounds on $W(s\boldsymbol{C}+\boldsymbol{G})$. There are two physically motivated properties we would like these bounds to have: if $s\boldsymbol{C}+\boldsymbol{G}$ is passive we would like $(s\boldsymbol{C}+\boldsymbol{G})^{-1}$ to be passive, and if $s\boldsymbol{C}+\boldsymbol{G}$ is stable we would like $(s\boldsymbol{C}+\boldsymbol{G})^{-1}$ to be stable. This is equivalent to saying that if the impedance representation of a circuit predicts stability, then its admittance representation should too.

The simplest bound on $W(\boldsymbol{A})$ is the rectangle defined by the Hermitian and anti-Hermitian parts of $\boldsymbol{A}$, see [12], [19], and Fig. 1. If $\boldsymbol{A}$ is positive definite, then $\boldsymbol{A}^{-1}$ is too. For a positive definite matrix, $\lambda_{\min}(\boldsymbol{A}_{\mathrm{H}}^{-1}) = 1/\lambda_{\max}(\boldsymbol{A}_{\mathrm{H}})$ and $\lambda_{\max}(\boldsymbol{A}_{\mathrm{H}}^{-1}) = 1/\lambda_{\min}(\boldsymbol{A}_{\mathrm{H}})$; thus, passivity is preserved in this approach. Unfortunately, stability is not.

If the bound in the preceding is viewed as rectangular, then what we need is a polar bound, although it will not be convex. The angular part of the bound is straightforward [20]; closely connected to $W(\boldsymbol{A})$ is $\Gamma(\boldsymbol{A}) \subset C$, the smallest convex cone that contains $W(\boldsymbol{A})$. For $\boldsymbol{A} \in C^{n\times n}$, we have

$$\Gamma(\boldsymbol{A}) \triangleq \{\boldsymbol{x}^{H}\boldsymbol{A}\boldsymbol{x} | \boldsymbol{0} \neq \boldsymbol{x} \in C^{n}\}. \tag{17}$$

From [20],

$$\Gamma(\boldsymbol{A}^{H}) = \Gamma(\boldsymbol{A}^{*}) = \Gamma^{*}(\boldsymbol{A}) = \Gamma(\boldsymbol{A}^{-1}) \tag{18}$$

where $\boldsymbol{A}^{*}$ denotes the complex conjugate of $\boldsymbol{A}$.

We also define two radii, r_{inner} and r_{outer}, where r_{outer} is the norm generally referred to as the numerical radius [21]. For a matrix $\boldsymbol{A} \in C^{n\times n}$,

$$r_{\mathrm{inner}} \triangleq \min\{|z| | z \in W(\boldsymbol{A})\} \tag{19}$$

and

$$r_{\mathrm{outer}} \triangleq \max\{|z| | z \in W(\boldsymbol{A})\}. \tag{20}$$

The bounds that we need are

Theorem 3: For $\boldsymbol{A} \in C^{n\times n}$ and $0 \notin W(\boldsymbol{A})$,

$$r_{\mathrm{outer}}(\boldsymbol{A}^{-1}) \leqslant \frac{1}{r_{\mathrm{inner}}(\boldsymbol{A})} \tag{21}$$

and

$$r_{\mathrm{inner}}(\boldsymbol{A}^{-1}) \geqslant \frac{r_{\mathrm{inner}}(\boldsymbol{A})}{4r_{\mathrm{outer}}^{2}(\boldsymbol{A})} \geqslant \left(\frac{r_{\mathrm{inner}}(\boldsymbol{A})}{2r_{\mathrm{outer}}(\boldsymbol{A})}\right)^{2} r_{\mathrm{outer}}(\boldsymbol{A}^{-1}). \tag{22}$$

Using these bounds, passivity and stability are both preserved under the operation of matrix inversion.

We are interested in the case where $0 \notin W(\boldsymbol{C})$. For $|s|$ sufficiently large, $0 \notin W(\boldsymbol{K}(s))$ (see Sections III and IV) and $r_{\mathrm{inner}} > 0$. We have

$$r_{\mathrm{inner}}(\boldsymbol{K}(s)) \geqslant |s| r_{\mathrm{inner}}(\boldsymbol{C}) - r_{\mathrm{outer}}(\boldsymbol{G}) \tag{23}$$

and

$$r_{\mathrm{outer}}(\boldsymbol{K}(s)) \leqslant |s| r_{\mathrm{outer}}(\boldsymbol{C}) + r_{\mathrm{outer}}(\boldsymbol{G}). \tag{24}$$

This leads to

$$r_{\mathrm{inner}}(\boldsymbol{K}^{-1}(s)) \geqslant \frac{|s| r_{\mathrm{inner}}(\boldsymbol{C}) - r_{\mathrm{outer}}(\boldsymbol{G})}{4(|s| r_{\mathrm{outer}}(\boldsymbol{C}) + r_{\mathrm{outer}}(\boldsymbol{G}))^{2}} \tag{25}$$

and

$$r_{\mathrm{outer}}(\boldsymbol{K}^{-1}(s)) \leqslant \frac{1}{|s| r_{\mathrm{inner}}(\boldsymbol{C}) - r_{\mathrm{outer}}(\boldsymbol{G})}. \tag{26}$$

Concentrating on r_{outer}, since $|s| \geqslant \omega$, (26) leads to

$$r_{\mathrm{outer}}(\boldsymbol{K}^{-1}(\sigma + j\omega)) \leqslant \frac{1}{\omega r_{\mathrm{inner}}(\boldsymbol{C}) - r_{\mathrm{outer}}(\boldsymbol{G})} \quad \text{for } \omega_{\max\text{-active}} > \frac{r_{\mathrm{outer}}(\boldsymbol{G})}{r_{\mathrm{inner}}(\boldsymbol{C})}. \tag{27}$$

Once $\omega > r_{\mathrm{outer}}(\boldsymbol{G})/r_{\mathrm{inner}}(\boldsymbol{C})$, the bound on $r_{\mathrm{outer}}(\boldsymbol{K}^{-1}(s))$ monotonically decreases toward zero with increasing ω.

When $\boldsymbol{K}^{-1}(s)$ is combined with a positive definite resistor $\boldsymbol{R}$, there exists a finite frequency $\omega_{\max\text{-active}}$ above which $\boldsymbol{Z}(s)$ is passive. Using (11), an upper bound on this frequency is given by the condition

$$\lambda_{\min}(\boldsymbol{R}_{\mathrm{H}}) = r_{\mathrm{outer}}(\boldsymbol{K}^{-1}(j\omega_{\max\text{-active}})) \quad \text{for } \omega_{\max\text{-active}} > \frac{r_{\mathrm{outer}}(\boldsymbol{G})}{r_{\mathrm{inner}}(\boldsymbol{C})}. \tag{28}$$

Theorem 4: Let $\boldsymbol{Z}(s) \in C^{n\times n}$ be an impedance matrix, as described in Theorem 1, where $\boldsymbol{Z}(s) = (s\boldsymbol{C}+\boldsymbol{G})^{-1} + \boldsymbol{R}$ and $\boldsymbol{C}, \boldsymbol{G}, \boldsymbol{R} \in R^{n\times n}$. If $0 \notin W(\boldsymbol{C})$ and $\boldsymbol{R}$ is positive definite, there exists a finite real frequency $\omega_{\max\text{-active}}$ above which $\boldsymbol{Z}(s)$ is passive. An upper bound on $\omega_{\max\text{-active}}$ is given by

$$\omega_{\max\text{-active}} \leqslant \frac{1}{r_{\mathrm{inner}}(\boldsymbol{C})}\left(\frac{1}{r_{\mathrm{inner}}(\boldsymbol{R})} + r_{\mathrm{outer}}(\boldsymbol{G})\right) \tag{29}$$

and $\sigma_{\max-\text{active}} < 0$ for

$$|\omega| \geq \frac{1}{r_{\text{inner}}(C)}\left(\frac{1}{r_{\text{inner}}(R)} + r_{\text{outer}}(G)\right). \qquad (30)$$

Note that this theorem does not require G passive or C symmetric. We require only that R be passive and $0 \notin W(C)$. Because $W(C)$ and $W(R)$ are convex and symmetric about the real axis, when C and R are positive definite, $r_{\text{inner}}(C) = \lambda_{\min}(C_H)$ and $r_{\text{inner}}(R) = \lambda_{\min}(R_H)$. Note also that $(\lambda^2_{\max}(G_H) + \lambda^2_{\max}(jG_{AH}))^{1/2} \geq r_{\text{outer}}(G) \geq \lambda_{\max}(G_H)$.

For the MOSFET model with nonreciprocal capacitances, R represents series drain and gate resistors—elements that actually exist in the physical device. The source and drain resistors are also present in simulation programs, notably SPICE2 [22], that use the nonreciprocal Ward model. (The Paulos model is not used because it is not a large-signal model.) We speculate that it is the presence of these resistors in the models implemented in the simulation program that prevents the widespread observation of "numerical" instability when these models are employed. Extremely high-frequency numerical noise, which one would otherwise suspect should be amplified by the dynamics of the Ward model, is attenuated and stabilized by the presence of series resistors. The maximum frequency of oscillation of the Ward model is quite sensitive to the values of the extrinsic parasitic resistors.

For the MOSFET model with reciprocal capacitors, the Paulos model shows the same qualitative behavior (at $\sigma = 0$) as one would expect for the Meyer model with series gate and drain resistors—at high frequency the numerical range moves into the right half-plane.

VI. Conclusion

Almost all of the early intrinsic MOSFET models [2]–[5] derived by simplifying *RC* transmission line models contain a series-gate resistor, which models the flow of the gate capacitive displacement current through the channel to the source. Somewhere along the line these series gate resistors were dropped, with the unfortunate result that $\omega_{\max-\text{active}} \to \infty$ for modern models of intrinsic MOSFET's. This is true both in the case of reciprocal and nonreciprocal capacitances. In the case of nonreciprocal capacitances, $\sigma_{\max-\text{active}}$ is not bounded either.

The behavior of MOSFET models that consist solely of a parallel multiport resistor and capacitor is fundamentally nonphysical. The maximum frequency of oscillation is infinite. This form of model should not be used for high-frequency simulation or analysis. The Ward and Paulos models represent the attempts to generate models that (among other things) improve on the high-frequency behavior of the Meyer model. Unfortunately, in the case of the Ward model, increased accuracy at low frequencies is achieved at the cost of violently nonphysical behavior at very high frequencies. The Paulos model appears to be better in this regard, although our theory is not yet general enough to tell the whole story.

Whereas non-quasi-static models of the sort investigated by Paulos and Antoniadis [18], Bagheri and Tsividis [23], and Chai and Paulos [24] represent one approach to extending the range of validity of MOSFET models in a way that does not appear to cause anomalous fundamental limits behavior, the author would like to suggest that reinserting the series gate resistor, which appeared in the early models [2]–[5] and was later inexplicably dropped, may provide a simple method for improving the accuracy and high-frequency behavior of MOSFET models.

Appendix
Proof of Theorems

Proof of Theorem 1: This theorem is a combination of theorems 1 and 4 of [9]. ■

Proof of Theorem 2: The proof follows from observing that $0 \in W(Y(s)) \Rightarrow 0 \in W(Y_H(s)) \Rightarrow Y(s)$ is not positive definite. ■

Proof of Theorem 3: It is convenient to use an equivalent definition for $W(A)$. For $A \in C^{n\times n}$ and $w, x \in C^n$,

$$W(A) = \left\{ \frac{w^H A w}{w^H w} \middle| 0 \neq w \in C^n \right\}.$$

Note the similarity to the definition of $\Gamma(\cdot)$ in (17). Since $0 \notin W(A)$, A is not singular and is hence invertible. Write $w = A^{-1}x$, where $w = 0$ iff $x = 0$. We have

$$W(A^H) = \left\{ \frac{x^H (A^{-1})^H A^H A^{-1} x}{x^H (A^{-1})^H A^{-1} x} \middle| 0 \neq x \in C^n \right\}.$$

This reduces to

$$W(A^H) = \left\{ \frac{x^H A^{-1} x}{x^H (A^{-1})^H A^{-1} x} \middle| 0 \neq x \in C^n \right\}.$$

From [21],

$$r_{\text{outer}}(A^{-1}) \leq \|A^{-1}\| \leq 2 r_{\text{outer}}(A^{-1})$$

where $\|A\|$ is the ordinary matrix norm of A.

Because $W(A^*) = W^*(A)$, we also have $r_{\text{inner}}(A) = r_{\text{inner}}(A^H)$ and $r_{\text{outer}}(A) = r_{\text{outer}}(A^H)$. Looking at $r_{\text{inner}}(A)$,

$$\begin{aligned} r_{\text{inner}}(A) &= r_{\text{inner}}(A^H) \\ &= \min_{x\neq 0} \left| \frac{x^H A^{-1} x}{x^H (A^{-1})^H A^{-1} x} \right| \\ &\geq \min_{x\neq 0} \left| \frac{x^H A^{-1} x}{\|A^{-1}\|^2 \|x\|^2} \right| \\ &\geq \min_{x\neq 0} \left| \frac{x^H A^{-1} x}{\|x\|^2} \right| \frac{1}{4 r^2_{\text{outer}}(A^{-1})} = \frac{r_{\text{inner}}(A^{-1})}{4 r^2_{\text{outer}}(A^{-1})}. \end{aligned}$$

Looking at $r_{\text{outer}}(A)$,

$$r_{\text{outer}}(A) = r_{\text{outer}}(A^{\text{H}}) = \max_{x \neq 0} \left| \frac{x^{\text{H}} A^{-1} x}{x^{\text{H}} (A^{-1})^{\text{H}} A^{-1} x} \right|$$

$$= \max_{x \neq 0} \frac{|x^{\text{H}} A^{-1} x|}{\|A^{-1} x\|^2}$$

$$\leqslant \max_{x \neq 0} \frac{\|x^{\text{H}}\| \|A^{-1} x\|}{\|A^{-1} x\|^2} = \max_{x \neq 0} \frac{\|x\|}{\|A^{-1} x\|}.$$

But $|x^{\text{H}} A^{-1} x| \leqslant \|x\| \|A^{-1} x\|$ so

$$\max_{x \neq 0} \frac{\|x\|}{\|A^{-1} x\|} \leqslant \max_{x \neq 0} \frac{\|x\|^2}{|x^{\text{H}} A^{-1} x|} = \frac{1}{r_{\text{inner}}(A^{-1})}. \quad \blacksquare$$

Proof of Theorem 4: Since this theorem concerns activity, we start by looking at $\lambda_{\min}((Z(s))_{\text{H}})$. We have

$$\lambda_{\min}\left((Z(s))_{\text{H}}\right) = \lambda_{\min}\left((K^{-1}(s) + R)_{\text{H}}\right)$$

$$\geqslant \lambda_{\min}\left((K^{-1}(s))_{\text{H}}\right) + \lambda_{\min}(R_{\text{H}}).$$

By relating the minimum eigenvalue of the Hermitian part to the numerical radius, we have

$$-r_{\text{outer}}(K^{-1}(s)) \leqslant \lambda_{\min}\left((K^{-1}(s))_{\text{H}}\right).$$

This, combined with (26), leads to

$$\lambda_{\min}(Z(s)) \geqslant r_{\text{inner}}(R_{\text{H}}) - \frac{1}{\sqrt{\omega^2+\sigma^2}\, r_{\text{inner}}(C) - r_{\text{outer}}(G)}.$$

Rearranging terms, we obtain

$$\sqrt{\omega^2 + \sigma^2} \leqslant \frac{r_{\text{inner}}(R) - r_{\text{inner}}(Z(\sigma + j\omega)) + r_{\text{outer}}(G)}{r_{\text{inner}}(C)}.$$

We can have $0 \in W(Z(s))$ or $0 \in W(Z_{\text{H}}(s))$ only if $\lambda_{\min}((Z(s))_{\text{H}}) \leqslant 0$. For this condition to be satisfied, we require

$$\sqrt{\omega^2 + \sigma^2} \leqslant \frac{r_{\text{inner}}(R) + r_{\text{outer}}(G)}{r_{\text{inner}}(C)}.$$

This reduces to (29) at $\sigma = 0$. For $\sigma > 0$, the ω at which natural frequencies can occur is reduced further. $\blacksquare$

REFERENCES

[1] A. Van Der Ziel and J. W. Ero, "Small-signal, high-frequency theory of field-effect transistors," *IEEE Trans. Electron Devices*, vol. ED-11, pp. 128–135, Apr. 1964.

[2] J. R. Hauser, "Small signal properties of field effect devices," *IEEE Trans. Electron Devices*, vol. ED-12, pp. 605–618, Dec. 1965.

[3] D. H. Treleaven and F. N. Trofimenkoff, "MOSFET equivalent circuit at pinch-off," *Proc. IEEE*, vol. 54, pp. 1223–1224, Sept. 1966.

[4] M. B. Das, "Generalized high-frequency network theory of field-effect transistors," *Proc. Inst. Elect. Eng.*, vol. 114, pp. 50–59, 1967.

[5] J. W. Haslett and F. N. Trofimenkoff, "Small-signal, high-frequency equivalent circuit for the metal-oxide-semiconductor field-effect transistor," *Proc. Inst. Elect. Eng.*, vol. 116, pp. 699–702, May 1969.

[6] J. E. Meyer, "MOS models and circuit simulation," *RCA Rev.*, vol. 32, pp. 42–63, Mar. 1971.

[7] D. E. Ward and R. W. Dutton, "A charge-oriented model for MOS transistor capacitances," *IEEE J. Solid-State Circuits*, vol. SC-13, pp. 703–707, Oct. 1978.

[8] L. A. Glasser, "Prediction of magnetic flux-controlled gate voltage in superconducting field-effect transistors," *IEEE Electron Device Lett.*, vol. EDL-10, pp. 82–84, Feb. 1989.

[9] ____, "Frequency limitations in circuits composed of linear devices," *IEEE Trans. Circuits Syst.*, vol. CAS-35, pp. 1299–1307, Oct. 1988.

[10] R. D. Thornton, D. DeWitt, P. E. Gray, and E. R. Chenette, *Characteristics and Limitations of Transistors*. New York: Wiley, chap. 3, 1966.

[11] R. D. Thornton, "Active RC networks," *IRE Trans. Circuit Theory*, vol. CT-4, pp. 78–89, Sept. 1957.

[12] A. I. Mees, *Dynamics of Feedback Systems*. New York: Wiley, p. 107, 1981.

[13] J. L. Wyatt, Jr., L. O. Chua, J. W. Gannett, I. C. Göknar, and D. N. Green, "Energy concepts in the state-space theory of nonlinear n-ports: Part I—Passivity," *IEEE Trans. Circuits Syst.*, vol. CAS-28, pp. 48–60, Jan. 1981.

[14] ____, "Energy concepts in the state-space theory of nonlinear n-ports: Part II—losslessness," *IEEE Trans. Circuits Syst.*, vol. CAS-29, pp. 417–430, July 1982.

[15] B. J. Sheu, W.-J. Hsu, and P. K. Ko, "An MOS transistor charge model for VLSI design," *IEEE Trans. Computer-Aided Design*, vol. 7, pp. 520–527, Apr. 1988.

[16] Y. P. Tsividis, *Operation and Modeling of the MOS Transistor*. New York: McGraw-Hill, 1987.

[17] P. Penfield, Jr., private communication.

[18] J. J. Paulos and D. Antoniadis, "Limitations of quasi-static models for the MOS transistor," *IEEE Electron Device Lett.*, vol. ED-4, pp. 221–224, July 1983.

[19] A. I. Mees and D. P. Atherton, "Domains containing the field of values of a matrix," *Linear Algebra Applications*, vol. 26, pp. 289–296, 1979.

[20] R. A. Horn and C. R. Johnson, *Topics in Matrix Analysis*. London, England: Cambridge University Press, 1988.

[21] P. R. Halmos, *A Hilbert Space Problem Book*. Princeton, NJ: Van Nostrand, p. 114, 1970.

[22] L. W. Nagel, "SPICE2: A computer program to simulate semiconductor circuits," Univ. California, Berkeley, ERL Memo. ERL-M520, May 1975.

[23] M. Bagheri and Y. Tsividis, "A small-signal dc-to-high frequency nonquasi-static model for the four-terminal MOSFET valid in all regions of operation," *IEEE Trans. Electron Devices*, vol. ED-32, pp. 2383–2391, Nov. 1985.

[24] K.-W. Chai and J. J. Paulos, "Comparison of quasi-static and non-quasi-static capacitance models for the four-terminal MOSFET," *IEEE Electron Device Lett.*, vol. ED-8, pp. 377–379, Sept. 1987.

✠

Lance A. Glasser received the B.S. degree in electrical engineering from the University of Massachusetts in Amherst in 1974, and the S.M. and Ph.D. degrees from the Massachusetts Institute of Technology in 1976 and 1979, respectively.

He is presently a Program Manager at the Defense Advanced Research Projects Agency. Before that, he spent one year as a Visiting Senior Researcher at Hitachi Central Research Laboratories. He was a member of the faculty in the Department of Electrical Engineering and Computer Science at the Massachusetts Institute of Technology from 1980 until 1988. He has published on microwave circuits and devices, picosecond optics, VLSI circuits and systems, CAD, and superconducting electronics. In addition to numerous articles and patents, he has written, with Dan Dobberpuhl, *The Design and Analysis of VLSI Circuits*, Addison-Wesley.

Dr. Glasser is the 1986 recipient of the ASEE Frederick Emmons Terman Award.